Biochemical and Biophysical Research Communications 456 (2015) 610–614

Contents lists available at ScienceDirect

Biochemical and Biophysical Research Communications

journal homepage: www.elsevier.com/locate/ybbrc

Alterations of urinary metabolite profile in model diabetic nephropathy

Donald F. Stec [a], Suwan Wang [b], Cody Stothers [b], Josh Avance [c], Deon Denson [d], Raymond Harris [b], Paul Voziyan [b,*]

[a] Vanderbilt Institute of Chemical Biology, Vanderbilt University Medical Center, Nashville, TN 37232, United States
[b] Department of Medicine, Vanderbilt University Medical Center, Nashville, TN 37232, United States
[c] Berea College, 1916 CPO, Berea, KY 40404, United States
[d] Choctaw Central High School, Philadelphia, MS 39350, United States

ARTICLE INFO

Article history:
Received 13 November 2014
Available online 10 December 2014

Keywords:
Urinary metabolites
Mouse models
Diabetic nephropathy
Nuclear magnetic resonance

ABSTRACT

Countering the diabetes pandemic and consequent complications, such as nephropathy, will require better understanding of disease mechanisms and development of new diagnostic methods. Animal models can be versatile tools in studies of diabetic renal disease when model pathology is relevant to human diabetic nephropathy (DN). Diabetic models using endothelial nitric oxide synthase (eNOS) knock-out mice develop major renal lesions characteristic of human disease. However, it is unknown whether they can also reproduce changes in urinary metabolites found in human DN. We employed Type 1 and Type 2 diabetic mouse models of DN, i.e. STZ-eNOS$^{-/-}$ C57BLKS and eNOS$^{-/-}$ C57BLKS *db*/*db*, with the goal of determining changes in urinary metabolite profile using proton nuclear magnetic resonance (NMR). Six urinary metabolites with significantly lower levels in diabetic compared to control mice have been identified. Specifically, major changes were found in metabolites from tricarboxylic acid (TCA) cycle and aromatic amino acid catabolism including 3-indoxyl sulfate, *cis*-aconitate, 2-oxoisocaproate, N-phenylacetylglycine, 4-hydroxyphenyl acetate, and hippurate. Levels of 4-hydroxyphenyl acetic acid and hippuric acid showed the strongest reverse correlation to albumin-to-creatinine ratio (ACR), which is an indicator of renal damage. Importantly, similar changes in urinary hydroxyphenyl acetate and hippurate were previously reported in human renal disease. We demonstrated that STZ-eNOS$^{-/-}$ C57BLKS and eNOS$^{-/-}$ C57BLKS *db*/*db* mouse models can recapitulate changes in urinary metabolome found in human DN and therefore can be useful new tools in metabolomic studies relevant to human pathology.

1. Introduction

A growing rate of diabetic kidney disease is one of the major pathologic consequences of diabetes pandemic [1]. Progression to end stage renal disease and accompanying cardiovascular complications are the primary causes of mortality in diabetic patients [2]. Introduction of new biomarkers to supplement microalbuminuria, which is currently used as the main indicator of kidney disease progression, should improve disease diagnosis and treatment. Active search for these biomarkers is underway involving genomic, transcriptomic, and proteomic technologies [3–5].

Several recent reports have demonstrated that metabolomics can be an important tool in identifying biomarkers of kidney disease and providing insights into pathogenic mechanisms [6–9]. In particular, urine metabolomics allows investigation of small biomolecules closely associated with kidney function or even originating from the kidney. In addition, urine is easier to collect and analyze compared to plasma, which is an important factor for potential clinical biomarker(s). Although metabolomic studies of diabetic kidney disease have been performed using mass spectrometry technology [6–9], proton NMR offers a number of advantages including minimal sample processing, high throughput, complete sample recovery, and direct structural identification of metabolites.

The results of several studies in animal models and human patients identified a number of urine metabolite biomarker candidates [6–8]. However, more studies utilizing different technologies

Abbreviations: DN, diabetic nephropathy; eNOS, endothelial nitric oxide synthase; NMR, nuclear magnetic resonance; TCA, tricarboxylic acid; ACR, albumin-to-creatinine ratio; STZ, streptozotocin; NOE, nuclear Overhauser effect; PCA, principal component analysis.

* Corresponding author at: Division of Nephrology, Vanderbilt University Medical Center, S-3223 MCN, 1161 21st Avenue South, Nashville, TN 37232-2372, United States. Fax: +1 615 343 7156.
E-mail address: paul.voziyan@vanderbilt.edu (P. Voziyan).

http://dx.doi.org/10.1016/j.bbrc.2014.12.003
0006-291X/

are needed to identify metabolite changes common to diabetic kidney disease. In particular, finding disease-related commonalities in metabolite profiles from human patients and animal models would facilitate use of versatile model tools to help searching for clinically relevant biomarkers. In this study, we utilized robust mouse models of Type 1 and Type 2 diabetic nephropathy (DN), which most fully reproduce pathologic lesions characteristic of human DN [10,11]. We employed ^{1}H NMR spectroscopy, which has previously been applied to studies of metabolites in diabetic plasma [12,13], to determine changes in urinary metabolite profiles in diabetic kidney disease.

We identified six urinary metabolites with significantly decreased levels in diabetic compared to control samples. These same six metabolites were showing similar changes in either Type 1 or Type 2 diabetic animal models. Levels of 4-hydroxyphenyl acetic acid and hippuric acid showed the strongest reverse correlation with the decline in renal function. Based on our findings in this study and on previous human studies [6,7], we conclude that STZ-eNOS$^{-/-}$ C57BLKS and eNOS$^{-/-}$ C57BLKS *db*/*db* mouse models can recapitulate changes in urinary metabolome found in human DN. We propose that these models can be important new experimental tools in metabolomic studies relevant to human pathology.

2. Materials and methods

2.1. Animal studies

In this study urine samples from three groups of mice were investigated: a control group and Type 1 diabetic and Type 2 diabetic groups (11 mice per group). Animal experiments were performed at the AAALAC-accredited animal facilities at Vanderbilt University Medical Center according to institutional guidelines and IACUC-approved experimental protocol. Mice were housed in an approved facility and given standard chow (Lab Diet 5015; PMI Nutrition International, Richmond, IN) and water *ad libitum*. For Type 1 diabetic model, 8 week old eNOS$^{-/-}$ C57BLKS were injected with low doses of STZ (50 mg/kg of BW) for 5 consecutive days to minimize potential toxic effects as previously described [11]. For the Type 2 diabetic model, we used eNOS$^{-/-}$ C57BLKS *db*/*db* mice [10]. Both models develop robust diabetic renal disease with pathologic lesions closely approximating those found in human DN [10,11]. Diabetic mice and age-matched wild type control mice were sacrificed at 20 weeks of age. Blood and spot urine were collected before sacrifice. Serum and urine samples were stored at −80 °C until analysis.

2.2. Determination of blood glucose and urinary albumin excretion

Glucose levels were measured in blood collected from the tail vein using OneTouch glucometer and Ultra test strips (LifeScan, Milpitas, CA) as previously described [10,11]. Albumin and creatinine excretion was determined in spot urine collected from individually caged mice using Albuwell-M kits (Exocell Inc., Philadelphia, PA) as previously described [10,11].

2.3. NMR experiments

NMR spectra were acquired using a 14.0 T Bruker magnet equipped with a Bruker AV-III console operating at 600.13 MHz. All spectra were acquired in 3-mm NMR tubes using a Bruker 5-mm TCI cryogenically cooled NMR probe operating at 298°K. Samples were prepared as 200 μL solutions that included 100 μL of urine, 41 μL of combination of 70 mM sodium phosphate buffer, TSP, and NaN_3, and 59 μL of 90/10% H_2O/D_2O which served as the ^{2}H lock solvent. TSP (3-(trimethylsilyl)propionic-2,2,3,3-d4 acid) in the buffer solution served as the zero ppm chemical shift reference.

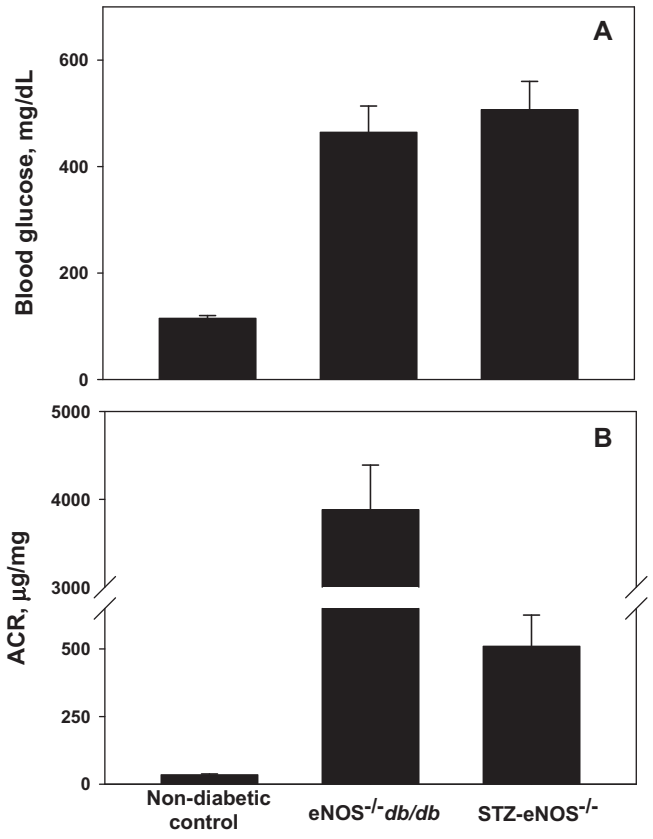

Fig. 1. Levels of blood glucose and albumin excretion in non-diabetic C57BLKS, eNOS$^{-/-}$ C57BLKS *db*/*db*, and STZ-eNOS$^{-/-}$ C57BLKS mice. Blood glucose (A) and urinary albumin-to-creatinine ratio (B) were determined in mice at 20 weeks of age as described under Section 2. Shown are means ± SEM; (n = 11).

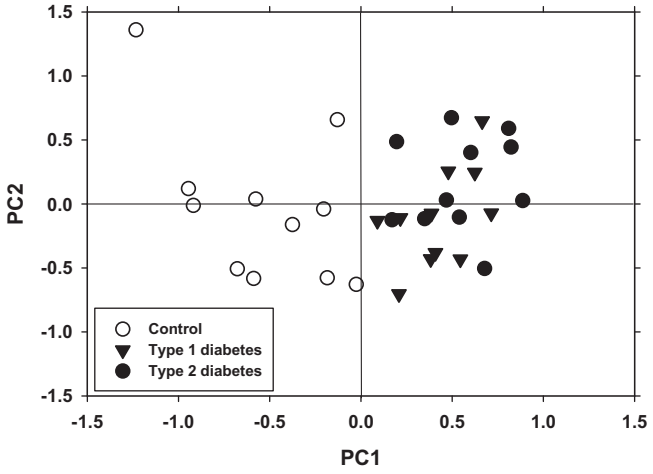

Fig. 2. Principal component analysis of the ^{1}H NMR data from control and diabetic urine samples. PCA scores were calculated using the data from control (*open circles*), diabetic Type 1 (*black triangles*) and diabetic Type 2 (*black circles*) urine samples as described under Section 2.

For 1D ^{1}H NMR, experiments were acquired using a one-dimensional nuclear Overhauser (1D-NOE) pulse sequence with presaturation solvent suppression to suppress the signal associated with water that is typically present in high concentration in mouse

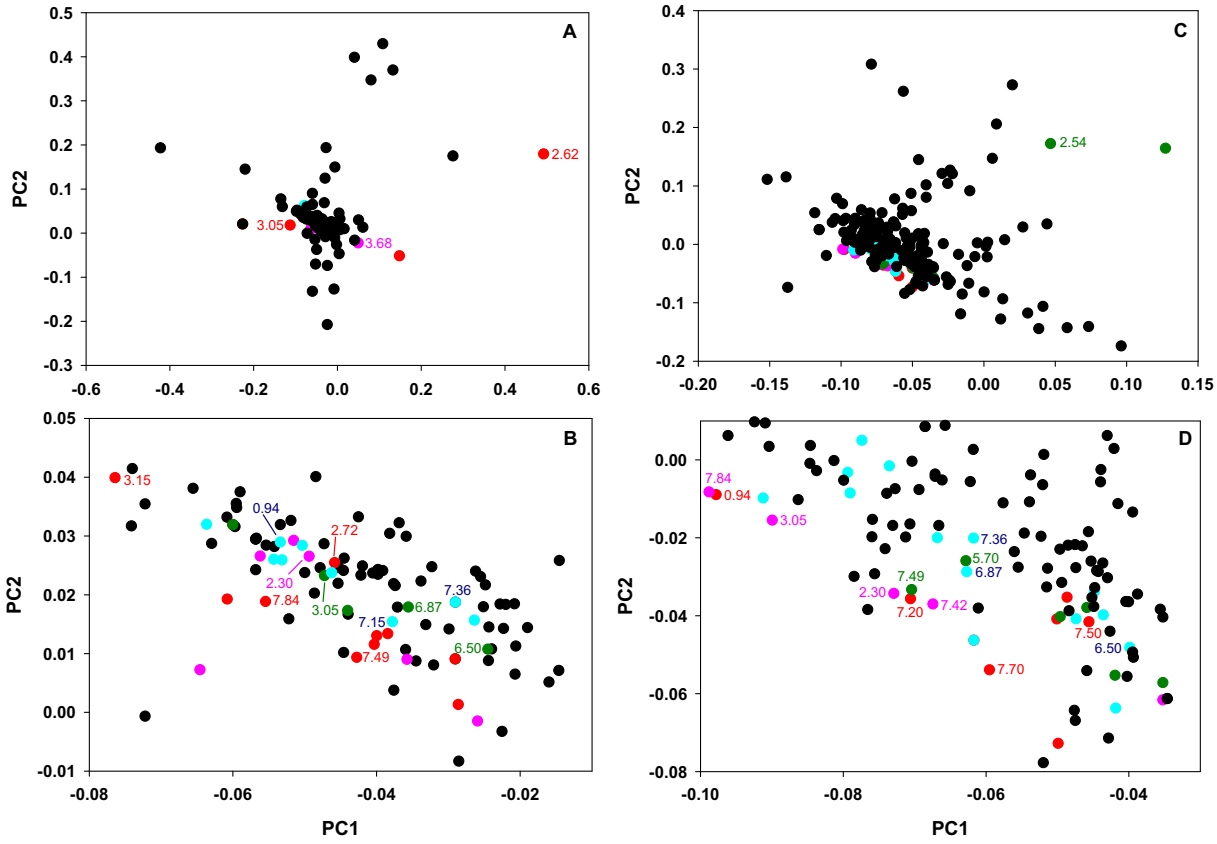

Fig. 3. Loadings plot of urinary metabolomics data from mouse models of Type 1 (A and B) and Type 2 (C and D) diabetes. (A and C) Heat maps are color-coded according to bucket *P* score values as described under Section 2. For the Type 1 diabetes data, the red points corresponded to $P < 8.3 \times 10^{-5}$, pink points: $8.3 \times 10^{-5} < P < 1.6 \times 10^{-4}$, green points: $1.6 \times 10^{-4} < P < 2.5 \times 10^{-4}$, blue points: $2.5 \times 10^{-4} < P < 3.2 \times 10^{-3}$ and black points: $P > 3.2 \times 10^{-3}$. For Type 2 diabetes data, red points corresponded to $P < 7.5 \times 10^{-5}$, pink points: $7.5 \times 10^{-5} < P < 1.8 \times 10^{-4}$, green points: $1.8 \times 10^{-4} < P < 5.0 \times 10^{-4}$, blue points: $5.0 \times 10^{-4} < P < 1.0 \times 10^{-3}$ and black points: $P > 1.0 \times 10^{-3}$. The numbers indicate ppm values of the selected NMR peaks with $P < 3 \times 10^{-3}$ for which metabolite assignments have been made. (B and D) Zoomed areas from the loadings plots in panels A and C, respectively. (For interpretation of the references to color in this figure legend, the reader is referred to the web version of this article.)

urine samples. The 1D-NOE experiment filters NMR signals associated with broad line widths such as those arising from proteins that might be present in urine samples and adversely affect spectral quality. Experimental conditions included: 32 K data points, 13 ppm sweep width, a recycle delay of 3 s, a mixing time of 150 ms and 32 scans.

2.4. NMR data analysis

Principal component analysis (PCA) was performed using the AMIX program (Bruker Biospin Corp., Billerica MA). This method requires NMR data to be distributed in chemical shift bins (0.01 ppm width) while eliminating the area associated with the water solvent suppression (4.6–5.1 ppm) and glucose (3.2–3.58, 3.62–4.108 and 5.22–5.276 ppm). Buckets with less than 5% variance were omitted prior to PCA. PCA reduces the dimensionality of the data and summarizes the similarities and differences between multiple NMR spectra using scores plots.

The statistical analysis of the NMR data was performed as previously published by Kennedy and co-workers [14]. The *P* scores were calculated and automatically divided into four groups by AMIX software based on significance level. These groups were color coded within PCA loadings plots according to *P* score values, thus generating a heat map representation of the data (Fig. 3). Buckets that corresponded to statistically significant *P* scores were compared to ppm values of the peaks that were identified from 1D & 2D NMR assignments. In order for a metabolite to be selected as a candidate, the occurrence of more than one metabolite peak had to be present in the statistically significant buckets. For example, 3-indoxyl sulfate was selected since the peaks at 7.70 and 7.49 ppm were among the buckets that appeared in the significant *P* score ranges for both the Type 1 and Type 2 data. Candidate metabolites were quantified by measuring the sum of the areas under all the characteristic resonance peaks corresponding to a given metabolite. Statistical analysis was performed using ANOVA followed by post hoc Tukey test. Statistical significance was determined after taking into account Bonferroni correction.

2.5. Identification of metabolites

Metabolites were identified by comparison of acquired spectra with standard spectra using the Chenomx Profiler program (Fig. S1). Metabolite identities were further confirmed using two dimensional ^{1}H–^{1}H COSY and ^{1}H–^{13}C HQSC (see Fig. S2 and Table S1 for spectral assignments). For 2D ^{1}H–^{1}H COSY, experimental conditions included 2048 × 512 data matrix, 13 ppm sweep width, recycle delay of 1.5 s and 8 scans per increment. The data were processed using squared sinebell window function, symmetrized, and displayed in magnitude mode. Multiplicity-edited HSQC experiments were acquired using a 1024 × 256 data matrix, a J(C–H) value of 145 Hz, which resulted in a multiplicity selection delay of 34 ms, a recycle delay of 1.5 s and 32 scans per increment along with GARP decoupling on ^{13}C during the acquisition time (150 ms). The data were processed using a $\pi/2$ shifted squared sine

Table 1
Levels of urinary metabolites in non-diabetic control and diabetic nephropathy model mice of Type 1 (STZ-eNOS$^{-/-}$) and Type 2 (eNOS$^{-/-}$ *db*/*db*) diabetes. Data presented as metabolite concentrations in urine of 20 week old mice, mean ± SEM. Relative metabolite levels represent integrated peak areas normalized to TSP standard. *P* values based on comparison of control vs. diabetic nephropathy groups ($n = 11$); Bonferroni-adjusted *P* value cut-off was 0.0056 to adjust for 9 metabolites; asterisk indicates significant change vs. control.

Metabolite	Proton NMR peak position (ppm)	Relative level in control urine	Relative level in Type 1 diabetic urine	*P* value vs. control	Relative level in Type 2 diabetic urine	*P* value vs. control
3-indoxyl sulfate	7.70, 7.49, 7.37, 7.20	1.48 ± 0.15	0.48 ± 0.06*	4.55E-05	0.24 ± 0.05*	7.78E-06
N-phenyl-acetylglycine	7.42, 7.36, 3.76, 3.68	3.29 ± 0.34	0.37 ± 0.03*	1.07E-05	0.48 ± 0.10*	8.25E-06
Cis-aconitate	5.70, 3.15	0.81 ± 0.08	0.079 ± 0.009*	1.07E-05	0.20 ± 0.03*	2.19E-05
2-oxoisocaproate	2.62, 2.09, 0.94	1.42 ± 0.21	0.24 ± 0.05*	1.79E-04	0.25 ± 0.06*	1.70E-04
4-hydroxyphenyl acetate	6.87, 7.15	0.36 ± 0.06	0.05 ± 0.01*	2.01E-04	0.04 ± 0.02*	1.73E-04
Hippurate	7.84, 7.64, 7.50, 3.95	1.81 ± 0.29	0.74 ± 0.11	0.017	0.63 ± 0.10*	0.004
2-oxoglutarate	3.05, 2.45	2.11 ± 0.47	0.95 ± 0.12	0.117	0.74 ± 0.17	0.033
Citrate	2.72, 2.54	3.57 ± 0.62	2.14 ± 0.35	0.217	2.81 ± 0.39	0.217
Fumarate	6.50	0.03 ± 0.01	0.03 ± 0.01	0.484	0.04 ± 0.01	0.217

window function and displayed with CH/CH_3 signals phased positive and CH_2 signals phased negative.

2.6. Statistical analyses

Mouse physiology data were expressed as means ± SEM; statistical analysis was performed using ANOVA followed by post hoc Tukey test. Differences were considered statistically significant if *P* values were less than 0.05.

3. Results and discussion

The two animal models of DN used in this study both exhibited hyperglycemia and, after about 14 weeks of diabetes, showed significantly increased urinary albumin excretion, indicative of renal damage (Fig. 1). Small molecule metabolites were analyzed in mouse urine using ^{1}H NMR spectroscopy. Principal component (PC) analysis of the NMR spectra revealed a clear separation of the data points into non-diabetic control and diabetic clusters (Fig. 2). This separation cannot be attributed to differences in glucose concentration between control and diabetic samples as glucose proton NMR signals were removed from the spectra before the analysis. Data from Type 1 and Type 2 diabetic mouse models clustered together in the PC plot indicating similarities of NMR spectra in these two models (Fig. 2).

In order to identify spectral features contributing to the observed data clustering, NMR spectra were divided into 0.01 ppm intervals (buckets) and signal intensities in each bucket were analyzed. The *P* score analysis using AMIX software identified multiple buckets with significant differences between control and diabetic samples (Fig. 3). This step provided for unbiased analysis of the spectral differences between the samples before the identities of specific metabolites were determined.

In the following metabolite identification step the ppm bucket values with significant *P* scores were used to identify only those individual urinary metabolites, whose levels significantly changed in diabetic compared to control urine samples. This analysis resulted in identification of nine candidate metabolite shown in Table 1 and in Table S2. Additional statistical analysis of integrated peak areas demonstrated that out of nine candidate metabolite identified from the loadings plot, only six metabolites were significantly decreased in diabetic vs. control urines (Table 1, top six entries) and levels of only five metabolites significantly correlated with urinary ACR, a marker of renal pathology (Table 2, top five entries). The most interesting finding was that urinary levels of hydroxyphenyl acetate and hippurate were significantly decreased in diabetes vs. control (Table 1) and also showed the strongest reverse correlation with ACR in diabetic mice (Table 2, top two entries). Reduction in glomerular filtration rate reported in diabetic

Table 2
Pearson correlation analysis of ACR vs. urinary metabolites in eNOS$^{-/-}$ *db*/*db* mice. Pearson correlation coefficient was determined for selected urinary metabolites identified in urine of Type 2 diabetic mice. Asterisks indicate significant correlation: $^*P < 0.05$ and $^{**}P < 0.01$ ($n = 11$).

Metabolite	Pearson correlation coefficient	*P* value
4-hydroxyphenyl acetate	−0.727	0.007**
Hippurate	−0.723	0.008**
3-indoxyl sulfate	−0.685	0.014*
2-oxoisocaproate	−0.621	0.031*
N-phenyl-acetylglycine	−0.599	0.040*
Cis-aconitate	−0.574	0.051
2-oxoglutarate	−0.413	0.183
Citrate	−0.367	0.241
Fumarate	−0.098	0.762

eNOS$^{-/-}$ C57BLKS *db*/*db* mice [10], is unlikely to significantly contribute to this phenomenon since several other small molecule urinary metabolites showed no correlation with ACR (Table 2). Thus, the decrease in hydroxyphenyl acetate and hippurate levels may reflect metabolic changes related to diabetes such as dysregulation of aromatic acid metabolism [15,16].

In order to confirm that our analyses identified all the detectable metabolites with significant changes between diabetic and control samples, we manually analyzed ^{1}H NMR spectra using Chenomx Profiler program. Although a total of twenty-three metabolites were thus identified (Table S3), no additional metabolites with significant changes in diabetic vs. control samples were found.

It is important to note that in this study using STZ-eNOS$^{-/-}$ C57BLKS and eNOS$^{-/-}$ C57BLKS *db*/*db* mouse models major changes were detected in urinary metabolites of aromatic amino acid catabolism, similar to those found in human DN [6,7]. Moreover, similar to our results urinary levels of hippuric and hydroxyphenyl acetic acids were also significantly decreased in human diabetic renal pathology as determined in mass-spectrometry based metabolomic studies [6,7]. In contrast, in *db*/*db* mouse model, major changes were detected in serum and urine metabolites of TCA cycle [8]. This finding is consistent with the fact that eNOS$^{-/-}$ *db*/*db* model more fully recapitulates major renal lesions found in human DN compared to the *db*/*db* model [10].

Compliance with ethical standards

Authors declare that they have no conflict of interest. All institutional and national guidelines for the care and use of laboratory animals were followed. No human studies were carried out by the authors for this article.

Acknowledgments

This work was supported by the grants DK65138 and DK51265 from the National Institutes of Health. Mr. Cody Stothers, Mr. Josh Avance, and Mr. Deon Denson were supported by the Vanderbilt Aspirnaut program and the grant 1R25DK096999 from the National Institutes of Health. We would also like to acknowledge the grant S10RR019022 from the National Institute of Health for funding the purchase of the 600 MHz NMR spectrometer used in this study.

Appendix A. Supplementary data

Supplementary data associated with this article can be found, in the online version, at http://dx.doi.org/10.1016/j.bbrc.2014.12.003.

References

[1] E.T. Rosolowsky, J. Skupien, A.M. Smiles, M. Niewczas, B. Roshan, R. Stanton, J.H. Eckfeldt, J.H. Warram, A.S. Krolewski, Risk for ESRD in type 1 diabetes remains high despite renoprotection, J. Am. Soc. Nephrol. 22 (2011) 545–553.

[2] P.H. Groop, M.C. Thomas, J.L. Moran, J. Waden, L.M. Thorn, V.P. Makinen, M. Rosengard-Barlund, M. Saraheimo, K. Hietala, O. Heikkila, C. Forsblom, The presence and severity of chronic kidney disease predicts all-cause mortality in type 1 diabetes, Diabetes 58 (2009) 1651–1658.

[3] K. Sharma, S. Lee, S. Han, B. Francos, P. McCue, R. Wassell, M.A. Shaw, S.P. RamachandraRao, Two-dimensional fluorescence difference gel electrophoresis analysis of the urine proteome in human diabetic nephropathy, Proteomics 5 (2005) 2648–2655.

[4] S.K. Iyengar, H.E. Abboud, K.A. Goddard, M.F. Saad, S.G. Adler, N.H. Arar, D.W. Bowden, R. Duggirala, R.C. Elston, R.L. Hanson, E. Ipp, W.H. Kao, P.L. Kimmel, M.J. Klag, W.C. Knowler, L.A. Meoni, R.G. Nelson, S.B. Nicholas, M.V. Pahl, R.S. Parekh, S.R. Quade, S.S. Rich, J.I. Rotter, M. Scavini, J.R. Schelling, J.R. Sedor, A.R. Sehgal, V.O. Shah, M.W. Smith, K.D. Taylor, C.A. Winkler, P.G. Zager, B.I. Freedman, Genome-wide scans for diabetic nephropathy and albuminuria in multiethnic populations: the family investigation of nephropathy and diabetes (FIND), Diabetes 56 (2007) 1577–1585.

[5] M.L. Alvarez, J.K. Distefano, The role of non-coding RNAs in diabetic nephropathy: potential applications as biomarkers for disease development and progression, Diabetes Res. Clin. Pract. 99 (2013) 1–11.

[6] K. Sharma, B. Karl, A.V. Mathew, J.A. Gangoiti, C.L. Wassel, R. Saito, M. Pu, S. Sharma, Y.H. You, L. Wang, M. Diamond-Stanic, M.T. Lindenmeyer, C. Forsblom, W. Wu, J.H. Ix, T. Ideker, J.B. Kopp, S.K. Nigam, C.D. Cohen, P.H. Groop, B.A. Barshop, L. Natarajan, W.L. Nyhan, R.K. Naviaux, Metabolomics reveals signature of mitochondrial dysfunction in diabetic kidney disease, J. Am. Soc. Nephrol. 24 (2013) 1901–1912.

[7] F.M. van der Kloet, F.W. Tempels, N. Ismail, R. van der Heijden, P.T. Kasper, M. Rojas-Cherto, R. van Doorn, G. Spijksma, M. Koek, J. van der Greef, V.P. Makinen, C. Forsblom, H. Holthofer, P.H. Groop, T.H. Reijmers, T. Hankemeier, Discovery of early-stage biomarkers for diabetic kidney disease using ms-based metabolomics (FinnDiane study), Metabolomics 8 (2012) 109–119.

[8] M. Li, X. Wang, J. Aa, W. Qin, W. Zha, Y. Ge, L. Liu, T. Zheng, B. Cao, J. Shi, C. Zhao, X. Yu, G. Wang, Z. Liu, GC/TOFMS analysis of metabolites in serum and urine reveals metabolic perturbation of TCA cycle in db/db mice involved in diabetic nephropathy, Am. J. Physiol. Renal Physiol. 304 (2013) F1317–1324.

[9] H. Abbiss, G.L. Maker, J. Gummer, M.J. Sharman, J.K. Phillips, M. Boyce, R.D. Trengove, Development of a non-targeted metabolomics method to investigate urine in a rat model of polycystic kidney disease, Nephrology (Carlton) 17 (2012) 104–110.

[10] H.J. Zhao, S. Wang, H. Cheng, M.Z. Zhang, T. Takahashi, A.B. Fogo, M.D. Breyer, R.C. Harris, Endothelial nitric oxide synthase deficiency produces accelerated nephropathy in diabetic mice, J. Am. Soc. Nephrol. 17 (2006) 2664–2669.

[11] Y. Kanetsuna, K. Takahashi, M. Nagata, M.A. Gannon, M.D. Breyer, R.C. Harris, T. Takahashi, Deficiency of endothelial nitric-oxide synthase confers susceptibility to diabetic nephropathy in nephropathy-resistant inbred mice, Am. J. Pathol. 170 (2007) 1473–1484.

[12] A.D. Maher, D. Crockford, H. Toft, D. Malmodin, J.H. Faber, M.I. McCarthy, A. Barrett, M. Allen, M. Walker, E. Holmes, J.C. Lindon, J.K. Nicholson, Optimization of human plasma 1H NMR spectroscopic data processing for high-throughput metabolic phenotyping studies and detection of insulin resistance related to type 2 diabetes, Anal. Chem. 80 (2008) 7354–7362.

[13] V.P. Makinen, P. Soininen, C. Forsblom, M. Parkkonen, P. Ingman, K. Kaski, P.H. Groop, M. Ala-Korpela, ^{1}H NMR metabonomics approach to the disease continuum of diabetic complications and premature death, Mol. Syst. Biol. 4 (2008) 167.

[14] A.M. Goodpaster, L.E. Romick-Rosendale, M.A. Kennedy, Statistical significance analysis of nuclear magnetic resonance-based metabonomics data, Anal. Biochem. 401 (2010) 134–143.

[15] E.A. Crandall, J.D. Fernstrom, Effect of experimental diabetes on the levels of aromatic and branched-chain amino acids in rat blood and brain, Diabetes 32 (1983) 222–230.

[16] C.J. Gibson, Diurnal alterations in retinal tyrosine level and dopamine turnover in diabetic rats, Brain Res. 454 (1988) 60–66.